Earthquake Engineering, Tenth World Conference © 1992 Balkema, Rotterdam. ISBN 90 5410 060 5

Dynamic analysis of impacting structural systems

J.P.Conoscente, R.O.Hamburger & J.J.Johnson
EQE Engineering, San Francisco, Calif., USA

ABSTRACT: Review of past earthquake damage shows that pounding of adjacent structures during earthquakes is a frequent phenomenon and an important cause of damage. Treatment of such impacts from an evaluation and design perspective has been somewhat limited in the past. Impact algorithms have focused on modeling impact by gap elements which rely on parameter estimations, such as gap element stiffness, which can significantly affect response. Project experience following the Loma Prieta earthquake led to the development and implementation of an energy based impact algorithm modeling the pounding of two buildings. The methodology and a numerical example from this study are presented.

1 INTRODUCTION

Past earthquake damage has shown that collision of adjacent buildings is one of the causes of severe structural damage in high density metropolitan areas located in seismically active regions. This problem has been most common in highly urbanized areas where maximization of land use has led to construction of adjacent buildings without adequate separations to avoid pounding. It has also been a problem for complexes of functionally interconnected structures, such as schools and hospitals, as well as for large or irregular structures provided with construction joints.

Generally, building codes require a minimum spacing between structures as a means of avoiding collision. However, this does nothing to address the hazard in existing constructions, nor to understand the effects pounding would create, nor to address the design practicality implications. This approach has major repercussions on the use of land in large urban areas, especially in California and Japan. This problem will become more acute throughout the world, as building codes for large metropolitan areas start implementing seismic design requirements.

Several studies of structural pounding have been undertaken in the past (Takayama 1973, Ban 1974, Miller 1980, Wolf 1980, Wada 1984, Maison 1990, SNL 1990, Stavroulakis 1991), but practical applications to date remain limited. Past developed approaches to study pounding model the impact as a stiff spring activated when the differential displacement between adjacent structures reaches a given clearance. This spring stiffness is a mathematical representation of a complicated phenomenon, but its value is not readily known, and it may significantly affect results (Maison 1990, SNL 1990).

In the course of investigating the effects of pounding for adjacent 15-story structures damaged by the Loma Prieta Earthquake, the authors have developed an algorithm for the analysis of pounding effects, using the physical laws of conservation of momentum and of energy. The technique is presented below, with an illustrative example.

2 DYNAMIC ANALYSIS OF TWO COLLIDING POINTS OF A SYSTEM

The dynamic analysis of two colliding points of a generalized system can be accomplished by applying the principle of the conservation of energy (Hamilton's principle) and the conservation of momentum.

2.1 Hamilton's principle

Hamilton's principle can be expressed as follows:

$$\int_{t-}^{t+}\delta(T-V)dt+\int_{t-}^{t+}\delta W_{nc}dt=0 \qquad (1)$$

For a closed (conservative) system, $\delta W_{nc} = 0$. Equation (1) can then be written as:

$$T(t^-) - V(t^-) = T(t^+) - V(t^+) \qquad (2)$$

The kinetic and potential energy of a system can be written as follows:

$$T(t) = 0.5 * \dot{y}^T(t) * M(t) * \dot{y}(t) \quad (3)$$

$$V(t) = 0.5 * y^T(t) * K(t) * y(t) \quad (4)$$

Combining equation (2) with (3) and (4) yields:

$$\dot{y}^T(t^-) * M(t^-) * \dot{y}(t^-) + y^T(t^-) * K(t^-) * y(t^-) = \dot{y}^T(t^+) * M(t^+) * \dot{y}(t^+) + y^T(t^+) * K(t^+) * y(t^+) \quad (5)$$

Assuming the mass and stiffness matrices remain constant over time, equation (5) can be written for a discretized system as follows:

$$\sum_{i=1}^{N} \sum_{j=1}^{N} \left[M_{ij} * \dot{y}_i(t^-) * \dot{y}_j(t^-) + K_{ij} * y_i(t^-) * y_j(t^-) \right] = \sum_{i=1}^{N} \sum_{j=1}^{N} \left[M_{ij} * \dot{y}_i(t^+) * \dot{y}_j(t^+) + K_{ij} * y_i(t^+) * y_j(t^+) \right] \quad (6)$$

2.2 Conservation of momentum

Conservation of momentum requires:

$$\Gamma(t^-) = \Gamma(t^+) \quad (7)$$

where:

$$\Gamma(t) = 1^T * M(t) * \dot{y}(t) \quad (8)$$

Assuming the mass matrix remains constant over time, equation (8) can be written for a discretized system as follows:

$$\sum_{i=1}^{N} \sum_{j=1}^{N} M_{ij} * \dot{y}_j(t^-) = \sum_{i=1}^{N} \sum_{j=1}^{N} M_{ij} * \dot{y}_j(t^+) \quad (9)$$

2.3 Impact analysis

The dynamic analysis of two impacting points in a MDOF system can thus be achieved by using equations (6) and (9).

Let k and l be the indices of the two impacting points. Since t^- and t^+ are respectively the instant right before impact and right after impact, the following relationships can be established:

$$\dot{y}_i(t^-) = \dot{y}_i(t^+) \text{ if } i \neq k \text{ and } i \neq l \quad (10)$$

$$y_i(t^-) = y_i(t^+) \text{ for all i between 1 and N} \quad (11)$$

Combining equations (6), and (11) thus yields:

$$\sum_{i=1}^{N} \sum_{j=1}^{N} M_{ij} * \dot{y}_i(t^-) * \dot{y}_j(t^-) = \sum_{i=1}^{N} \sum_{j=1}^{N} M_{ij} * \dot{y}_i(t^+) * \dot{y}_j(t^+) \quad (12)$$

For lumped mass systems, Mij = 0 if $i \neq j$. For these systems, equations (12) and (9) can be simplified as:

$$\sum_{i=1}^{N} M_i * \dot{y}_i(t^-) = \sum_{i=1}^{N} M_i * \dot{y}_i(t^+) \quad (13)$$

$$\sum_{i=1}^{N} M_i * \dot{y}_i(t^-)^2 = \sum_{i=1}^{N} M_i * \dot{y}_i(t^+)^2 \quad (14)$$

Combining equation (10) with equations (13) and (14) produces:

$$M_k * \dot{y}_k(t^-)^2 + M_l * \dot{y}_l(t^-)^2 = M_k * \dot{y}_k(t^+)^2 + M_l * \dot{y}_l(t^+)^2 \quad (15)$$

$$M_k * \dot{y}_k(t^-) + M_l * \dot{y}_l(t^-) = M_k * \dot{y}_k(t^+) + M_l * \dot{y}_l(t^+) \quad (16)$$

This system of equations can be rearranged as:

$$M_k * [\dot{y}_k(t^-)^2 - \dot{y}_k(t^+)^2] = M_l * [\dot{y}_l(t^+)^2 - \dot{y}_l(t^-)^2] \quad (17)$$

$$M_k * [\dot{y}_k(t^-) - \dot{y}_k(t^+)] = M_l * [\dot{y}_l(t^+) - \dot{y}_l(t^-)] \quad (18)$$

Solution for this system can be easily obtained. Eliminating the trivial solution $\dot{y}_k(t^-) = \dot{y}_k(t^+)$ and $\dot{y}_l(t^-) = \dot{y}_l(t^+)$, equations (17) and (18) can be rewritten as follows:

$$M_k * [\dot{y}_k(t^-) - \dot{y}_k(t^+)] = M_l * [\dot{y}_l(t^+) - \dot{y}_l(t^-)] \quad (19)$$

$$\dot{y}_k(t^-) + \dot{y}_k(t^+) = \dot{y}_l(t^+) + \dot{y}_l(t^-) \quad (20)$$

which are the equations for the impact of two particles.

The coefficient of restitution c_r (Harris 1988) is defined as:

$$c_r = [\dot{y}_l(t^+) - \dot{y}_k(t^+)] / [\dot{y}_l(t^-) - \dot{y}_k(t^-)] \quad (21)$$

For an inelastic shock, equation (20) can be written:

$$\dot{y}_l(t^+) - \dot{y}_k(t^+) = -c_r * [\dot{y}_l(t^-) - \dot{y}_k(t^-)] \quad (22)$$

Combining equations (19) and (22) gives the solution:

$$\dot{y}_i(t^+) = \frac{M_l * \dot{y}_l(t^-) + M_k * \dot{y}_k(t^-) - c_r * M_k * [\dot{y}_l(t^-) - \dot{y}_k(t^-)]}{M_l + M_k} \quad (23)$$

$$\dot{y}_k(t^+) = \frac{M_i * \dot{y}_i(t^-) + M_k * \dot{y}_k(t^-) + c_r * M_i * [\dot{y}_i(t^-) - \dot{y}_k(t^-)]}{M_i + M_k} \quad (24)$$

Equations (10), (23) and (24) yield the velocities after impact of the impacting degrees of freedom. In a step-by-step integration solution, Equation (11) yields their displacements.

Consider, the equations of motion for each building:

$$M*\ddot{y}(t)+C*\dot{y}(t)+K*y(t) = F(t) \quad (25)$$

The solution process proceeds in two steps. First, the equations of motion for each building are transformed to modal coordinates:

$$y(t) = \sum_{n=1}^{NM} \Phi_n * q_n(t) \quad (26)$$

and the common properties of orthogonality uncouple the resulting equations of motion. Second, the known portion of the solution at time t is transformed to the right hand side supplementing the load vector. Of course, the known values of accelerations, velocity, and displacement for the impacting degrees of freedom are transformed into modal coordinates, also, yielding:

$$[\ddot{q}_n(t)+2\zeta w_n \dot{q}_n(t)+w_n^2 q_n(t)]_{unknown} = F_n(t)-[\ddot{q}_n(t)+2\zeta w_n \dot{q}_n(t)+w_n^2 q_n(t)]_{known} \quad (27)$$

The solution for this equation can be easily obtained by modal time integration solution. The advantages are obvious -- no concern with artificial impact elements and the ability to represent the impact by physical parameters such as coefficient of restitution. Also, the algorithm is very fast computationally and can be easily implemented in existing structural analysis programs because it uses linear modal superposition.

3 ILLUSTRATIVE EXAMPLE

The algorithm described above was implemented in the program MODSAP (Johnson 1976) to analyze the seismic response of impacting structures. As an illustration, two adjacent 15-story buildings are evaluated for structural pounding. Both buildings are steel frame structures with concrete shear walls, and are about 46 m by 49 m in plan. Equivalent stick models of the two structures were constructed. The two structures have marginal clearance in the X direction. This configuration is typical of functionally interconnected structures constructed in phases.

Frequencies for the first five modes of each building are given in Table 1. Building 2 is about 20% more massive and is stiffer than Building 1. Most of the structural response of both buildings is captured by the first ten modes of each building.

Mode	Bldg 1	Bldg 2
1	0.67	0.81
2	0.93	1.03
3	1.59	2.12
4	2.23	3.06
5	3.07	3.48

Table 1. First five undamped frequencies (Hz)

For demonstration purposes, impact is monitored only at the top floor, and can only occur in the X-direction. Preliminary analysis of the two buildings showed that impact would occur at a ground motion level of approximately 0.15g. To analyze the effects of a severe earthquake, the seismic input level was set at 0.40g and a three-dimensional time history analysis of both structures was performed. Response spectra of the input time histories are shown in Figure 1.

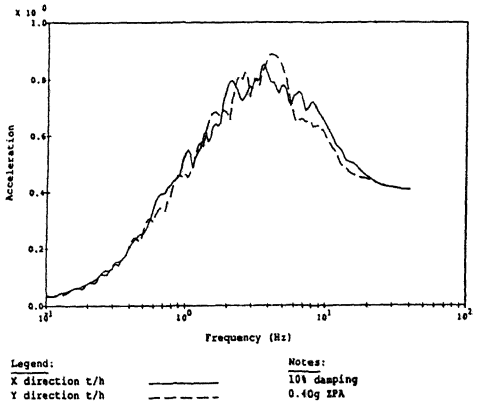

Figure 1. Response spectra of input time histories

To evaluate the sensitivity of the results, several gap sizes were studied. The uncoupled response of the buildings (assuming no impact occurs) were compared with the coupled response of the buildings including impact. Response was measured as maximum story shears. This comparison allows a better understanding of the significance of pounding loads on structural response. Impact amplification factors were calculated as the ratio of the maximum

story shear for the given time history at 0.40g PGA, to the scaled maximum story shears resulting by scaling the linear results for 0.15g PGA to 0.40g PGA. Two gaps were considered: 10 and 5 cm. Results for the impact amplification factors are summarized in Table 2. Both cases were performed for a coefficient of restitution of 1.0 (elastic shock).

FLOOR	10 CM GAP		5 CM GAP	
BLD 1	X	Y	X	Y
15	2.406	1.001	2.769	1.006
14	1.860	1.001	2.151	1.001
13	1.162	1.001	1.238	0.998
12	1.141	1.001	1.040	0.996
11	1.109	1.001	1.107	0.994
10	1.201	1.001	1.334	0.993
9	1.071	1.001	1.215	0.992
8	1.066	1.001	1.007	0.995
7	1.074	1.001	1.028	0.995
6	1.077	1.000	1.048	0.994
5	1.064	1.000	1.055	0.994
4	1.038	0.999	1.038	0.993
3	1.083	0.999	1.033	0.993
2	1.111	0.993	1.054	0.992
1	1.140	0.993	1.160	0.992
BLD 2	X	Y	X	Y
15	1.959	0.989	2.777	0.963
14	1.754	0.989	2.545	0.962
13	1.389	0.988	2.135	0.962
12	0.973	0.988	1.562	0.963
11	0.987	0.988	1.028	0.966
10	1.001	0.989	0.968	0.967
9	1.001	0.996	0.967	0.984
8	1.000	0.995	0.967	0.985
7	0.999	0.995	0.966	0.985
6	0.998	0.995	0.965	0.986
5	0.997	0.995	0.963	0.990
4	0.997	0.996	0.961	0.996
3	0.983	0.996	0.950	1.002
2	0.979	0.980	0.941	0.994
1	0.989	0.964	0.944	0.983

Table 2. Impact amplification factors

These results indicate that for these two structures, building response is mostly uncoupled for the two orthogonal directions. In addition, they show that the pounding effects are localized and that the story shears are dramatically affected for floors near the top story where impact was assumed; in this case yielding story shears amplification factors of up to 3. The X-direction displacement time histories of the top floor of each building are superimposed on Figure 2. When the two curves of Figure 2 touch each other, the two buildings are colliding. The gap size is also shown to have a significant effect on individual story shears. For instance, a reduction in gap size from 10 to 5 cm increases the maximum story shear by a factor of 1.5 at the top floor of building 2. This might be due to the fact that the velocities developed with a 5 cm gap are greater than those with a 10 cm gap. As the structures are further and further apart, the energy transferred at impact is smaller and smaller. However, gaps smaller than 5 cm might also yield smaller impact ratios because rattling will prevent the systems from developing high velocities.

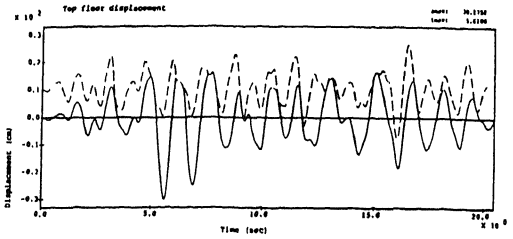

Figure 2. Displacement of the top floors of two adjacent structures, 10 cm apart

The analysis presented here serves only as an illustration of the methodology. However, the general trends are certainly applicable to other problems, such as the influence of pounding on the structural response, and the sensitivity to the size of the clearance.

4 CONCLUSION

Pounding of adjacent buildings has been documented as a cause of life-threatening structural damage in several recent earthquakes. Building codes have responded to this observation by requiring that new construction be adequately separated to prevent interaction from occurring or designed to account for the resulting impact forces and response modifications. However, this does nothing to address the hazard in existing conditions or the practicality of separating functionally interconnected structures. A new approach based on energy balance and modal analysis is presented for the general treatment of pounding of structures. This approach is efficient and can be easily implemented since it uses linear modal superposition. In addition, it does not require an estimation of an equivalent spring stiffness which is not readily known but may affect results.

An illustrative example is presented using this approach. The results indicate the story shears are dramatically affected by impact but that these effects are localized in the areas of impact and can therefore be accounted for in a retrofit or initial design. Limited parametric studies were performed to illustrate the importance of gap distances. Other parameters, such as coefficient of restitution, relative floor mass, input time histories, and soil-structure interaction will also affect the structural pounding response, and their importance should be investigated in future research.

5 APPENDIX I. REFERENCES

Blan, S. (1974). "Collision of Adjacent Buildings Due to Earthquake Excitation". Trans. Architectural Institute of Japan, 221, 1-7.

Clough, R.W., Penzien, J. (1975). "Dynamics of Structures", McGraw-Hill Book Company, 189-194.

Harris, C.M. (1988). "Shock and Vibration Handbook", 3rd ed., McGraw-Hill Book Company, 9.1-9.11.

Johnson, J.J. (1976). "MODSAP, A Modified Version of the Structural Analysis Program SAP IV for the Static and Dynamic Response of Linear and Localized Nonlinear Structures", National Technical Information Service, GA-A14006.

Maison, B.F., Kasai, K. (1990). "Analysis for Type of Structural Pounding". Journal of Structural Engineering, ASCE, 116(4), 957-977.

Miller, R.K. (1980). "Steady Vibroimpact at a Seismic Joint Between Adjacent Structures". Proceedings of the Seventh World Conference on Earthquake Engineering. International Association of Earthquake Engineering.

Sandia National Laboratories, Westinghouse Hanford Company, EQE Incorporated, ERCE Incorporated (1990). "Analysis of Core Damage Frequency Due to External Events at the Department of Energy N- Reactor". SAND89-1147.

Stavroulakis, G., Abdalla, K. (1991). "Contact Between Adjacent Structures". Journal of Structural Engineering, Vol. 117, No. 10.

Takayama, K. (1973). "Earthquake Response of a Building Collided with a Neighboring Building". Proceedings of the Fifth World Conference on Earthquake Engineering. International Association of Earthquake Engineering, 2, 2211-2214.

Uniform Building Code (1988). International Conference of Building Officials. Whittier, CA.

Wada, A., Shinozaki, Y., Nakamura, N. (1974). "Collapse of Buildings with Expansion Joints Through Collision Caused By Earthquake Motion". Proceedings of the Eighth World Conference on Earthquake Engineering. International Association of Earthquake Engineering.

Wolf, J.P., Skrikerud (1980). "Mutual Pounding of Adjacent Structures During Earthquakes". Journal of Nuclear Engineering Design, 57, 253-275.

6 APPENDIX II. NOTATIONS

The following symbols are used in this paper:

C = Damping matrix;
ζ_n = Modal damping ratio for mode n;
c_r = Coefficient of restitution;
$F(t)$ = Load vector at time t;
$F_n(t)$ = Modal load vector for mode n at time t;
K = Stiffness matrix; $= [K_{ij}]$;
M = Mass matrix; $= [M_{ij}]$;
Φ_n = Mode shape vector for mode n;
$q_n(t)$ = Modal displacement vector for mode n at time t;
$y(t)$ = Relative displacement vector at time t;
$\dot{y}(t)$ = $\frac{dy(t)}{dt}$
w_n = Circular undamped frequency of mode n.
T = Kinetic energy of system.
V = Potential energy of system.
δ = variation taken during indicated time interval.
W_{nc} = Work done by non-conservative forces acting on system.
t^- = Instant right before impact occurs.
t^+ = Instant right after impact occurs.
$\Gamma(t)$ = Momentum of system at time t
1^T = { 1, 1, ..., 1}, 1xN vector
N = Number of degrees-of-freedom
NM = Number of modes